Supplementary Information for:

Amyloid Aggregation on Lipid Bilayers and its Impact on Membrane Permeability

Ran Friedman, Riccardo Pellarin and Amedeo Caflisch

Department of Biochemistry, University of Zürich, Winterthurerstrasse 190, CH-8057 Zürich, Switzerland

December 17, 2008

I. Computational Methods

1 Simulation protocols

1.1 Set-up of the molecular dynamics simulations

The simulations were carried out as follows. First, a conformation taken from a 1-μs simulation of 1000 lipid molecules, where a single bilayer vesicle had formed spontaneously, is positioned in the center of a cubic box (l=290Å). Then, 125 peptides are added to the box, corresponding to a concentration of 8.5mM, which allows the comparison with previous studies [1, 2]. Furthermore, the critical concentration for micelle formation of the model peptides is 4.3mM, and it is therefore preferable to use higher concentration of peptides in the simulations. Each peptide is placed at a random position, at least 15Å away from any other molecule and outside of the vesicle (see Figure 1(b) of the main text). The initial conformation of the peptide (i.e., π or β) is taken from a distribution corresponding to dE. For example, for dE=0.0 kcal/mol, approximately half of the molecules are in either state, whereas for dE=-1.5 kcal/mol only about 11 of the 125 peptides are in the β state. The system is then energy-minimized by 150 steps of the steepest-descent and 200 steps of the conjugate-gradient algorithm. After minimization,

the temperature of the system is gradually increased to 310K over 10000 steps of MD simulation with a timestep of 2fs, before equilibration for further 10000 steps at constant temperature. A second equilibration phase of 10000 steps is initiated with Langevin dynamics, allowing a longer timestep of 50fs. The friction in the Langevin simulations is determined by a coefficient of 0.01 ps^{-1}. To make sure that the internal degrees of freedom equilibrate properly, a single bead of each molecule is kept fixed during this phase. Following equilibration, a production Langevin dynamics run is initiated with non of the beads fixed. All simulations are carried out with the computer program CHARMM [7], version 31. The simulations were continued until the number of inter-molecular contacts between polar atoms did not increase anymore (1μs of simulation time, or 2μs for dE=-2.0), as a constant number of polar contacts indicates that the aggregation state of the peptides is constant [1]. A 1-μs run with 1000 lipids and 125 peptides requires about 2 weeks on a single core of a Xeon 5345 at 2.33 GHz. Each system was simulated at least 10 times, with different random seeds for the initial distribution of velocities and peptide monomers. The total number of simulations is given in Table S1. Simulations without lipids were carried out as detailed in [1].

2 Visual presentation and analysis

Figures of snapshots from the simulations were prepared by the computer program VMD [9]. Analysis was carried out by home written software and by analysis programs from the Gromacs simulation package, version 3.3.3 [10, 11]. A modified version of the computer program Wordom [12] was used to convert the CHARMM trajectories to a format that can be handled by Gromacs. The analysis program g_clustsize was modified to allow the study of lipid or peptide clusters. A cutoff of 6Å was used for clustering.

2.1 The number of peptides attached to the vesicle

The use of a strict cutoff may lead to artifacts when calculating the number of peptides attached to the vesicle surface (as presented in Figure 3 of the main text). Consider, for example, a fibril

of 100 peptides which is located at minimal distances of 6.3, 5.9, and 6.8Å from the vesicle at simulation frames $i-1$, i, and $i+1$, respectively. Although the fibril is not attached to the vesicle, the calculated number of peptides from the vesicle will show a sharp increase by 100 at a frame i. To avoid such spurious discontinuities the number of peptides attached to the vesicle at each frame, $n_{pept}(i)$ was compared with that of the preceding frame $n_{pept}(i-1)$. If the difference (in absolute value) was larger than 20, we set $n_{pept}(i) = n_{pept}(i-1)$ unless the new value persists for 5ns or more. In other words, if the condition:

$$|n_{pept}(i+j) - \ n_{pept}(i)| < 20$$

holds for each j such that $t(i+j) - t(i) \leq 5ns$ then the value of $n_{pept}(i)$ is not modified.

2.2 Polar contacts between the peptides

The degree of fibrillation can be quantified by the number of polar contacts between the peptides [1]:

$$n_p = \sum_{i,j=1;i\neq j}^{125} [\theta(d_{contact} - r_{ij}^{A2,A6}) + \theta(d_{contact} - r_{ij}^{A3,A10})]$$

where $d_{contact}$=5Å, θ is the Heaviside step function, which is zero or one if the argument is negative or positive, respectively, and A2, A3, A6 and A10 are the dipole bead types (see Figure S1). The maximal number of polar contacts is twice the number of peptides, i.e., 250. However, in the final stage of the simulations there is an equilibrium between fibrils and unbound peptide monomers, and the number of polar contacts is therefore smaller (200-230).

2.3 Calculation of the number of probes inside vesicles

The number of probes within the vesicle interior is evaluated using the technique of ray-tracing [13]. Six "rays", corresponding to the positive and negative cartesian directions, are cast from the center of every probe. If all six rays are colliding with any peptide or lipid atom, then the probe is deemed to be in the vesicle interior. Operationally, given the position (x_i^P, y_i^P, z_i^P) of

probe i, and the position (x_k^a, y_k^a, z_k^a) of atoms belonging to peptides and lipids, the projections over the planes (x, y), (x, z) and (y, z) of the distance between the probe i and atom k are defined as

$$r_{i,k}^{\rho} = ((\mu_k^a - \mu_i^P)^2 + (\nu_k^a - \nu_i^P)^2)^{1/2}$$

where $(\mu, \nu) = (x, y)$ if $\rho = z$, (x, z) if $\rho = y$, and (y, z) if $\rho = x$. The number of non-colliding rays cast from probe i, N_i^r, is obtained by the following sum:

$$N_i^r = \sum_{\rho=x,y,z} \left[\prod_k \theta(\rho_k^a)\theta(r_{i,k}^{\rho} - r_{coll}) + \prod_k \theta(-\rho_k^a)\theta(r_{i,k}^{\rho} - r_{coll}) \right]$$

where θ is the Heaviside step function, *vide ante*. In this work the collision distance r_{coll} is set to 3.5 Å, a value that gives a good signal to noise ratio. Probe i is considered to be in the vesicle if N_i^r is equal to zero. The number of probes in the vesicle, $n_{prob,in}$, is:

$$n_{prob,in} = \sum_{i=1}^{20} \delta(N_i^r)$$

where the value of Kronecker δ function is one if its argument is zero and zero otherwise.

II. Supplementary Table

λ^a	**Amyloidogenicity**^{b}	**Number of simulations**	**Fibrillation** $\mathbf{t_{50}^c}\pm$**s.d. [ns]**	**Leakage** $\mathbf{t_{50}^d}\pm$ **s.d [ns]**
0.87	high	10	11 ± 1	123 ± 89
	intermediate	29	89 ± 29	175 ± 124
	low^e	20	958 ± 503	444 ± 178
	very low	30	>1000	503 ± 171
0.90	high	10	10 ± 1	167 ± 89
	intermediate	30	69 ± 23	168 ± 88
	low	30	>1000	321 ± 154
	very low	10	>1000	331 ± 161

Table S1: Simulation details, including characteristic half-times for fibrillation and leakage, presented for two λ values. The simulations were run for 1μs unless otherwise stated. ^{a} The multiplicative parameter λ scales the Lennard-Jones interaction energy between peptides and lipids, thereby modulating the affinity of the peptides for the bilayer. Note that the variations in fibrillation rates are magnified when the interactions between the lipids and the peptides are stronger. ^{b}Amyloidogenicity is determined by dE. A value of dE=0 kcal/mol corresponds to high amyloidogenicity, -1.5 to intermediate, -2.0 to low and -2.25 to very low. The parameters dE and λ are completely independent. ^{c}The rate of fibrillation is quantified by the half time of fibril formation, t_{50}. t_{50} is defined as the simulation time required for the formation of a fibril with 100 polar contacts, since there are 200-250 polar contacts between the peptides (each peptide can make two polar contacts with adjacent peptides and the total number of peptides in the simulations is 125). ^{d}The average time needed for 50% of the probes to escape from the vesicle.

III. Supplementary Figures

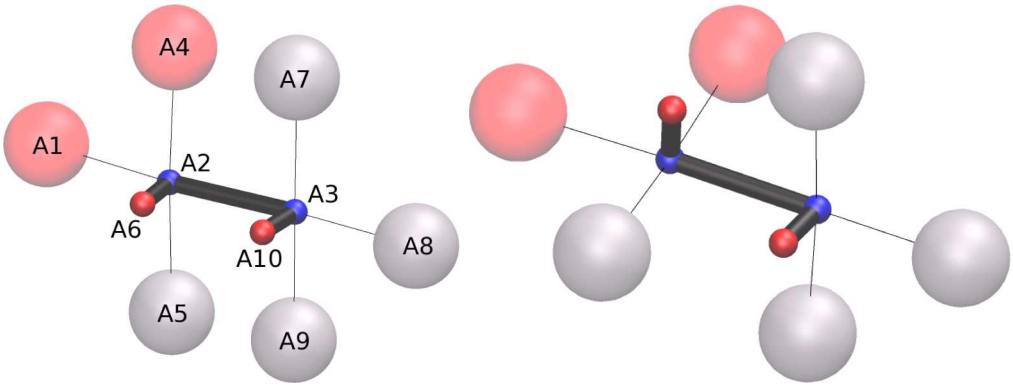

Figure S1: The peptide model. The beads carrying partial charges are shown in blue (+0.4e) and red (-0.4e). Hydrophilic, uncharged beads are shown in gray, hydrophobic beads in light red. The β state is shown on the left, the π on the right. Note the different orientation of the dipoles. The parameter dE is the energy difference E_π - E_β. Each bead has a mass of 1000 Da. For more information about the model, see [1].

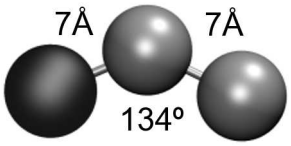

Figure S2: The lipid model. The hydrophobic and hydrophilic beads are presented in light and dark gray, respectively. Each bead has a mass of 250 Da.

References

[1] Pellarin, R. & Caflisch, A. Interpreting the aggregation kinetics of amyloid peptides. *J Mol Biol* **360**, 882–892 (2006).

[2] Pellarin, R., Guarnera, E. & Caflisch, A. Pathways and intermediates of amyloid fibril formation. *J Mol Biol* **374**, 917 – 924 (2007).

[3] Cooke, I. & Deserno, M. Solvent-free model for self-assembling fluid bilayer membranes: stabilization of the fluid phase based on broad attractive tail potentials. *J Chem Phys* **123**, 224710 (2005).

[4] Ryckaert, J.-P., Ciccotti, G. & Berendsen, H. J. C. Numerical integration of the cartesian equations of motion of a system with constraints: Molecular dynamics of n-alkanes. *J Comput Phys* **23**, 327–341 (1977).

[5] Lopes, D. *et al.* Mechanism of islet amyloid polypeptide fibrillation at lipid interfaces studied by infrared reflection absorption spectroscopy. *Biophys. J.* **93**, 3132–3141 (2007).

[6] Aisenbrey, C. *et al.* How is protein aggregation in amyloidogenic diseases modulated by biological membranes? *Eur Biophys J* **37**, 247–55 (2008).

[7] Brooks, B. R. *et al.* Charmm: A program for macromolecular energy, minimization, and dynamics calculations. *J. Comp. Chem.* **4**, 187–217 (1983).

[8] Engel, M. F. M. *et al.* Membrane damage by human islet amyloid polypeptide through fibril growth at the membrane. *Proc. Natl. Acad. Sci. U.S.A.* **105**, 6033–6038 (2008).

[9] Humphrey, W., Dalke, A. & Schulten, K. VMD: visual molecular dynamics. *J. Mol. Graph.* **14**, 33–38 (1996).

[10] Berendsen, H. J. C., van der Spoel, D. & Vandrunen, R. Gromacs - a message-passing parallel molecular-dynamics implementation. *Comput. Phys. Commun.* **91**, 43–56 (1995).

[11] Lindahl, E., Hess, B. & van der Spoel, D. Gromacs 3.0: A package for molecular simulation and trajectory analysis. *J. Mol. Mod.* **7**, 306–17 (2001).

[12] Seeber, M., Cecchini, M., Rao, F., Settanni, G. & Caflisch, A. Wordom: a program for efficient analysis of molecular dynamics simulations. *Bioinformatics* **23**, 2625–2627 (2007).

[13] Spencer, G. H. & Murty, M. V. R. K. General Ray-Tracing Procedure. *J. Opt. Soc. Am.* **52**, 672–8 (1961).